Published in final edited form as:
Curr Biol. 2011 March 8; 21(5): 345–352. doi:10.1016/j.cub.2011.01.039.

Signaling in the Arabidopsis shoot meristem stem cell niche correlates with ligand-dependent trafficking of the CLV1 receptor kinase

Zachary L. Nimchuk, **Paul T. Tarr**, **Carolyn Ohno**, **Xiang Qu**, and **Elliot M. Meyerowitz**[$]
Division of Biology 156-29, California Institute of Technology, Pasadena, CA 91125. USA

Summary

Cell numbers in above-ground meristem types of plants are thought to be maintained by a feedback loop driven by perception of the glycopeptide ligand CLAVATA3 (CLV3) by the CLAVATA1 (CLV1) receptor kinase and the CLV2/CORYNE (CRN) receptor-like complex [1]. CLV3 made in the stem cells at the meristem apex limits the expression level of the stem cell-promoting homeodomain protein WUSCHEL (WUS) in the cells beneath, where *CLV1* as well as *WUS* RNA are localized. WUS downregulation nonautonomously reduces stem cell proliferation. High-level overexpression of CLV3 eliminates the stem cells and causes meristem termination [2], and loss of CLV3 function allows meristem overproliferation [3]. There are many open questions regarding the CLV3/CLV1 interaction, including where in the meristem it occurs, how it is regulated, and how it is that a large range of CLV3 concentrations gives no meristem size phenotype [4]. Here we use genetics and live imaging to examine the cell biology of CLV1 in *Arabidopsis* meristematic tissue. We demonstrate that plasma membrane-localized CLV1 is reduced in concentration by CLV3, which causes trafficking of CLV1 to lytic vacuoles. We find that changes in CLV2 activity have no detectable effects on CLV1 levels. We also find that CLV3 appears to diffuse broadly in meristems, contrary to a recent sequestration model which states that CLV3 is quantitatively bound by CLV1 in the apical regions of the meristem, allowing continued WUS activity in lower regions [5]. This study provides a new model for CLV1 function in plant stem cell maintenance and suggests that downregulation of plasma membrane-localized CLV1 by its CLV3 ligand can account for the buffering of CLV3 signaling in the maintenance of stem cell pools in plants.

Introduction

Post-embryonic growth in higher plants is driven by populations of meristematic cells that are continuously maintained over the life of the plants. In plants like *Arabidopsis*, above-ground tissues are derived from the shoot apical meristem (SAM), which begins as a vegetative meristem making leaves, then becomes an inflorescence meristem (IM) that bears determinate floral meristems (FM), from which the reproductive organs are derived. These diverse meristematic forms share a common tissue organization composed of a stem cell population called a central zone at the apical meristem tip, above a set of cells sometimes

[$]author for correspondence: meyerow@caltech.edu.

called the organizing center or rib meristem, and flanked by a peripheral zone in which organs form. This identity organization is overlaid upon a tissue pattern consisting of clonal monolayers of L1 and L2 cells overlying the corpus cell population. Mutations in any of the *CLV*/*CRN* loci result in an overproliferation of stem cells in shoot meristems. Mutations in the homeodomain protein WUSCHEL result in a premature termination of the stem cell population [6]. *CLV3* encodes a small extracellular protein which is processed into a 13 amino acid peptide and modified with β-1,2-linked tri-arabinoside chains into its active *in vivo* form (CLV3p, [7–9]). It is thought that the mature CLV3p diffuses from its expression domain in the upper meristem layers into deeper tissue layers where CLV1 is expressed [10]. CLV1 is a transmembrane receptor kinase with extracellular leucine-rich repeats that can bind CLV3p in vitro [10,11]. Binding is thought to activate CLV1 kinase activity which in turn leads to a downregulation of *WUS* expression in the rib meristem. WUS can activate *CLV3* expression in a cell non-autonomous manner, thereby providing a mechanistic feedback loop which maintains stem cell balance [2,12]. In addition, a parallel CLV3p sensing pathways involving the receptor-like protein CLV2 and the receptor-like kinase homologue CRN also regulates stem cell proliferation via *WUS* [13,14]. *CLV2*/*CRN* is expressed broadly and this complex is proposed to act as a receptor for a diverse set of CLV3-related ligands, termed CLE proteins, throughout the plant [1]. In addition, the receptor kinase RPK2/TOAD2 also acts to limit *WUS* expression in the meristem[15]. Because it is thought that *CLV1* and *WUS* could be expressed in overlapping cell populations in the meristem, it has been proposed that CLV1 may act to prevent the diffusion of CLV3 into the entire *WUS* domain by sequestering CLV3p [5]. Although high levels of ectopic *CLV3* can downregulate *WUS*, alteration of *CLV3* levels over a wide range are buffered by unknown mechanisms in the meristem [4]. In addition, long-term expression of high levels of CLV3 can lead to reactivation of *WUS* [4], suggesting that strict controls upon the perception of CLV3 exist in plants. What these control mechanisms are and how they relate to the function of the various receptors is unknown.

Our knowledge of how these loci interact to control stem cell function is derived from genetic, biochemical and transient expression imaging studies. However the literature contains several contradictions. For example, past biochemical studies suggested that CLV2 is required for stabilization of CLV1, with a 90% reduction in CLV1 levels seen in *clv2-1* null plants [16]. This result does not appear to be compatible with the genetic observation that *clv2 clv1* and *crn clv1* double mutants are additive [14,15,17]. Attempts to image CLV1 and associated proteins in living meristems have until now been unsuccessful.

Here we use a combination of genetic analysis and live confocal imaging of CLV1-reporters to explore the cell biology of CLV1 in living meristematic tissue. We observe that CLV1 accumulates at the plasma membrane (PM) in *clv3* plants and is preferentially targeted to the lytic vacuole by CLV3. These results indicate that CLV3 promotes ligand-dependent trafficking of the CLV1 receptor kinase, analogous to the ligand dependent downregulation of receptors in animal systems and at least one plant receptor like kinase (RLK) [18]. Endosomal trafficking and lysosomal degradation of receptors in animal and yeast cells provides a mechanism for downregulation of activated receptors [19]. In some cases receptors signal from endosomal compartments providing strict temporal and spatial regulation of pathway activation [20]. Trafficking of CLV1 likely requires meristem-specific cofactors. We demonstrate that *CLV2* is neither required for CLV3-dependent trafficking of CLV1 nor is it required for stabilization of CLV1 in *clv3* plants. These results call into question the validity of some biochemical studies, but are consistent with genetic analyses of the loci. Using trafficking of CLV1 as a marker for CLV3 perception we are able to ascertain that CLV3 appears to diffuse broadly in the meristem and that sequestration of CLV3 by CLV1 is therefore unlikely to play a major role in meristem maintenance. These

data provide a new model for CLV1/CLV3 interactions and suggest that downregulation of CLV1 by CLV3 could provide the CLV3 buffering function observed in previous work.

Results

CLV1 accumulates at the plasma membrane in *clv3* mutants

In order to study the cell biology of CLV1-CLV3 interactions we first created a *CLV1* promoter construct to express CLV1-2xGFP for live imaging (Supplemental Experimental Procedures, Supplemental Figure 1). This construct fully complemented the *clv1-11* and *clv1-101* mutants in all lines examined (n>30) (Supplemental Figure 1 A and B). This fusion protein localizes to the PM in tobacco transient expression experiments (data not shown). In contrast to the results in tobacco we rarely observed PM localization of CLV1-2xmGFP in the IMs in T1 transgenic plants. Instead we observed in most cases a faint GFP signal in the vacuole of L3 cells. In other cases, we observed faint apparently cytosolic background signal (compare Figure 1C and Figure 2A and C, Supplemental Figure 2 for imaging controls). In animal systems, receptors are internalized and degraded in response to ligand binding and we postulated that we might be observing a similar process in the case of CLV1. We introgressed a single insert line of *pCLV1::CLV1-2xGFP* into the *clv1-11 clv3-2* background, which is RNA null for both *CLV1* and *CLV3* [21, 22]. We compared young lateral IMs as these were the closest in size and shape between the two genotypes. We observed the same weak apparent vacuolar accumulation and lack of PM GFP signal in *CLV3* progeny in rib meristem cells as in a wild-type genetic background (Figure 1A and 1C). In *clv3-2* progeny, however, we observed GFP signal at the presumed PM in rib meristem cells and a corresponding lack of vacuolar accumulation (Figure 1B and 1D). In both genotypes (*clv1-11 clv3-2* and *clv1-11 CLV3*) we observed punctate structures in the cytosol which are likely Golgi apparatus (see Supplemental Experimental Procedures). We confirmed these results by introgressing a separate *clv1-11 pCLV1::CLV1-2xGFP* line into the *clv1-11 clv3-2* background and repeating the earlier observations (Supplemental Figure 3). This line complements but expresses at a much lower level. In this line we never observed PM accumulation in the IMs in *CLV3* plants. These data indicate that in the absence of CLV3, CLV1 accumulates at the PM, while it is found in the vacuole in the presence of CLV3 protein (see Supplemental Material). This suggests that CLV3 drives CLV1 endocytosis from the PM followed by subsequent targeting to the vacuole. Both CLV1 and CLV3 are also expressed in young FMs arising from the flanks of the main IM. In stage 3 FMs, CLV1-2xGFP localization was largely similar to that of the main IM (Supplemental Figures 4 and 6). In general, levels of CLV1-2xGFP appeared higher in FMs compared to IMs when expressed from *pCLV1*, although this may be due to partial shadowing of the IM by peripheral FMs. On rare occasions (3/20 experiments) we observed weak CLV1-GFP signal at the PM in FMs of *CLV3* plants, however CLV1-GFP PM signal was always higher in *clv3* mutants in those same experiments. In a separate survey of 21 individual *CLV1:CLV1-2xYpet CLV3* transgenic lines we did not detect any PM localization in FMs, further confirming that PM accumulation of CLV1 is strongly reduced in the *CLV3* background.

We then expressed the CLV1-2xGFP fusion at high level in all cells of the IM. We generated a *pUBQ::CLV1-2xGFP* construct and transformed *clv1-11*, *clv3-2 clv1-11*, and *clv1-101* plants. Constitutive expression of *CLV1* complemented the *clv1* null phenotype without any other observed effects (Supplemental Figure 1F). We introgressed three individual *pUBQ::CLV1-2xGFP* lines, two *clv1-11* lines and one *clv1-101* line, into *clv3-2 clv1-11* plants and analyzed progeny in a similar manner to the above *pCLV1* experiments. Consistent with the imaging of the *pCLV1::CLV1-2xGFP* lines, we observed a strong vacuolar accumulation in *CLV3* plants and a contrasting strong PM accumulation in *clv3-2* plants (Figure 2). The vacuolar signal derived from the *pUBQ10* lines was considerably

stronger than that seen in most, but not all, *pCLV1* imaging attempts. Similar results to those with *pCLV1::CLV1-2xGFP* were obtained from the introgression of two other independent *pUBQ::CLV1-GFP* lines, one in the *clv1-101* background (Figure 2A and 2B) and another in *clv1-11*, into the *clv3-2 clv1-11* plants (Figure 2C and 2D, detail shown). In very high level expressing IMs, we occasionally noticed weak PM accumulation of CLV1 in the *CLV3* background from *pUBQ* and *pCLV1* lines (Figure 2C, data not shown), suggesting that CLV1 may saturate downstream trafficking components at very high levels. Variation at *ERECTA* did not affect CLV1-2xGFP localization in either *clv3* or *CLV3* backgrounds (Figure 2, data not shown). These results confirm that CLV3 promotes vacuolar localization of CLV1 at the expense of PM accumulation.

CLV1 traffics to the lytic vacuole in VTI11-dependent manner

We confirmed the localization of CLV1 in *CLV3* and *clv3* plants using known markers for the PM and lytic vacuole respectively (Suppl. data and methods). To further test the hypothesis that CLV3 alters CLV1 trafficking, we took a genetic approach and crossed the *pCLV1::CLV1-2xGFP* transgene into a *zig-1* mutant background. *ZIG/VTI11* encodes a Q-SNARE protein which localizes to the Trans-Golgi Network/Pre-Vacuolar Compartment (TGN/PVC) and is required for transport of cargo to the lytic vacuole [23–26]. In *zig-1 CLV3* plants the CLV1-2xGFP vacuolar signal was greatly reduced compared to *ZIG CLV3* plants in most experiments, indicating that CLV1 is trafficked to the lytic vacuole in a ZIG/VTI11-dependent manner in *CLV3* plants (Figure 3A and B). We consistently observed a stronger PM accumulation of CLV1-2xGFP signal in *zig-1 CLV3* plants that is rarely seen in *ZIG CLV3* plants. We noted that upon prolonged FM4-64 staining in *CLV3* plants, internal CLV1-2xGFP was bounded by FM4-64 stained tonoplast (Figure 3C). We also observed colocalization of CLV1-2xGFP signal with two known lytic vacuole markes, LysoTracker Red and the vacuolar RFP marker (VAC-RFP, Figure 3D and E, see Supplemental Experimental Procedures), confirming the vacuolar targeting of CLV1-2xGFP in *CLV3* plants. We confirmed the localization of CLV1 in *clv3* plants via colocalization with PM targeted mRUBY and FM4-64 staining in cold treated plants (Figure 4, Supplemental Figure 4, Supplemental Experimental Procedures).

Ectopic CLV1 does not sequester CLV3

CLV3 is expressed in the L1, L2 and L3 layers in wild type plants. From there it is believed that the CLV3 pro-peptide is secreted to the extracellular space where it is processed and modified with L-arabinose into its active 13 amino acid glycopeptide form, CLV3p [8]. It is not known where CLV3p diffuses and is active in the shoot apical meristem. Previous attempts to define the sites to which CLV3 diffuses in the IM used a CLV3-GFP fusion [5,7]. Later studies demonstrated that CLV3p is proteolytically cleaved from its precursor at both its amino-terminal and carboxyl-terminal ends, indicating that the CLV3-GFP in these earlier experiments likely reported only the extracellular movement of the processed GFP and not the active CLV3p. Using *UBQ::CLV1-2xGFP* lines and vacuolar trafficking of CLV1-2xGFP as a proxy for the CLV3p response of CLV1, we determined that CLV3p diffuses broadly throughout the IM from its site of synthesis (Figure 3 A and B,Figure 5). We observed *CLV3*-dependent vacuolar accumulation of CLV1-2xGFP throughout the L1 layer, in the peripheral zone and central zone, and also in deeper regions encompassing the rib meristem. We also consistently observed *CLV3*-dependent vacuole targeting in young flower primordia, suggesting that CLV3 may either diffuse across the boundary regions or be synthesized in low levels in emerging primordia. It has been proposed that CLV1 protects lower regions of the IM from CLV3 by sequestering CLV3 and preventing its diffusion [2]. *CLV1* is normally expressed at higher levels in the rib zone of IMs, and its RNA is largely absent from the L1 and L2 layers. We tested this sequestration hypothesis using high level ectopic expression of *CLV1*, including in the L1, L2 and L3 layers in the *pUBQ* lines. We

found that CLV1 overexpression in L1 and L2 cells did not prevent perception of CLV3p by CLV1 in the lower central zone and in the rib meristem as judged by the vacuolar targeting of CLV1-2xGFP in L3 and L4 cells (Figure 5). In addition, lateral epidermal L1 cells on the flanks of the IM still showed response to CLV3. These cells would be expected to be even further from the site of CLV3 than L3 cells. This observation suggests that functional sequestration of CLV3p by CLV1 doesn't occur to a detectable degree in the L3 layer of wild type meristems. These results are also consistent with the observation that meristem function is unperturbed over a wide range of *CLV3* levels [4] and the lack of *wus*-like phenotypes seen in any combination of *clv1* heterozygotes [21,27].

CLV3 is sufficient to promote CLV1 vacuolar trafficking

We sought to assess whether it was sufficient to induce CLV1-2xGFP trafficking in shoot apical meristems. We generated *DEX::CLV3 clv3-2* plants in which constitutive *CLV3* expression is inducibly controlled by the application of dexamethasone (DEX) in the *clv3-2* background (Supplemental Materials and Methods). In control *clv3-2 pUBQ::CLV1-2xGFP* plants and untreated *clv3-2 pUBQ::CLV1-2xGFP DEX::CLV3* plants we observed the expected PM accumulation of CLV1-2xGFP in L1 cells in young IMs (Figure 6 top row and bottom row). In contrast, *clv3-2 pUBQ::CLV1-GFP DEX::CLV3* plants treated with DEX for several days displayed a range of CLV1-2xGFP localizations. While some IMs displayed near normal levels of CLV1-2xGFP at the PM in L1 cells (data not shown), others displayed a strong vacuolar accumulation similar to that seen in the *CLV3 pUBQ::CLV1-2xGFP* plant lines (Figure 6, upper middle row). Others yet displayed greatly reduced CLV1-2xGFP signal at the PM (Figure 6, lower middle row), yet still expressed CLV1-2xGFP strongly in the epidermis of mature sepals (data not shown). Neither of the latter observations were ever seen in control treated *clv3-2 pUBQ::CLV1-GFP DEX::CLV3* plants. These results indicate that CLV3 is sufficient to induce both PM depletion and drive trafficking of CLV1 to the lytic vacuole. Vacuolar accumulation of the CLV1-GFP signal was first weakly detected at 4 hours post DEX application in two independent experiments, suggesting that this response was relatively rapid. These data demonstrate that CLV3 is both necessary and sufficient to drive depletion of CLV1 from the PM in apical meristems, followed by trafficking to the lytic vacuole in a post-transcriptional manner.

We never observed strong vacuolar targeting of CLV1-2xGFP in DEX-treated tissues outside of meristems in *pUBQ::CLV1-GFP DEX::CLV3* plants, consistent with the robust PM accumulation of CLV1-2xGFP in the mature sepal epidermis of *CLV3 pUBQ::CLV1-GFP* plants (data not shown, Supplemental Experimental Procedures). This observation suggests that CLV1 requires meristem-specific cofactors in order to traffic to the vacuole in response to CLV3. Also consistent with this, we observed no changes in CLV1-2xGFP vacuolar targeting in response to either CLV3p or *DEX::CLV3* in transient tobacco leaf transformation assays (data not shown).

CLV2 is not required for CLV1 stability or trafficking

Previously, it has been published that *CLV2* is required for CLV1 stability, with a reduction in CLV1 levels by 90% in *CLV3 clv2* plants relative to wild type [16]. As described in the introduction, several lines of evidence challenge these data and conclusions. We therefore sought to address what role, if any, CLV2 might play in CLV1 levels or cellular location. We crossed both *pCLV1::CLV1-2xGFP* and *pUBQ::CLV1-2xGFP* plant lines into a *clv1-11 clv2-1 clv3-2* triple mutant, which is protein-null for CLV2 as a result of a stop codon at amino acid position 33 in the *CLV2* signal sequence [16] and selected the appropriate F2 genotypes. We observed a similar pattern of CLV1-2xGFP signal in *pUBQ* lines, with reduced PM accumulation in the *pUBQ* lines and significant vacuolar targeting in *CLV3 CLV2* and *CLV3 clv2-1* plants (Figure 7A). These data demonstrate that loss of CLV2 does

not impair CLV3-dependent lytic vacuole targeting. Similarily, CLV1 levels and PM targeting appeared unchanged the *clv3-2 CLV2* and *clv3-2 clv2-1* backgrounds (Figure 7B). . Similar results were also seen in both IMs and stage 3 FMs from *pCLV1* lines (Supplemental Figures 5 and 6). We also did not detect a reduction in CLV1-2xGFP levels in the *clv2-1* mutant by Western Blot analysis (Supplemental figure 7B). These data indicate that CLV2 is not required for the stability or accumulation of GFP-labeled CLV1.

Discussion

The experiments reported here suggest a new model for CLV1 function. In the absence of CLV3, CLV1 accumulates at the PM. In this model CLV3p is secreted from L1/L2 and some L3 cells and diffuses into to the *CLV1* expression domain. Ligand binding triggers activation of the CLV1 kinase, which in turn causes recruitment of accessory proteins, resulting in CLV1 internalization from the PM followed by VTI11/ZIG-dependent trafficking to the lytic vacuole, where CLV1 is degraded. It seems unlikely that quantitative sequestration of CLV3 by CLV1 occurs, as is currently believed, because CLV3 has an effect on the subcellular localization of CLV1 through much of the IM, even when CLV1 is overexpressed. Although *WUS*, *CLV3* and *CLV1* have never been colocalized simultaneously in the same plant, recent *in situ* hybridizations suggest that *CLV3* expression partially overlaps with that of *WUS* in meristems [28].

We did not observe robust changes in CLV1 protein levels between *CLV3* and *clv3-2* plants. Similar results have been seen for FLS2 and S-Receptor kinase (S. Robatzek, personal communication, and [29]). It could be that any changes in CLV1 levels are masked by CLV1 levels outside of these cells, for example in vascular tissues, where CLV1 is present. Alternatively the amount of PM CLV1 in *clv3* plants might be roughly equivalent to the sum of CLV1 in vesicles in *CLV3* plants. Clearly some CLV1 must always be present at the PM in wild-type plants in order to perceive CLV3. Consistent with this in highly expressing IMs and FMs we do observe weak accumulation of CLV1 at the PM in *CLV3* plants suggesting that the efficacy of CLV1 trafficking is sensitive to CLV1 levels.

The results reported here demonstrate that CLV1 accumulates at the PM in both shoot and floral meristems, and traffics to the lytic vacuole in a ZIG/VTI11-dependent manner. This appears to differ from the RLK STRUBBELIG, which accumulates at the PM in a domain overlapping with that of *CLV1* in IMs [30]. Interestingly, the stem cell limiting RLK RPK2 appears to be post translationally downregulated in IMs similar to CLV1 [15], suggesting it may also undergo ligand dependent trafficking. While trafficking to the vacuole is reduced in *CLV3 zig-1* mutants, we also observe a consistent accumulation of CLV1-2xGFP at the PM in *CLV3 zig-1* IMs. This may reflect an increase in CLV1 recycling to the PM when vacuolar targeting is reduced. This would be consistent with the known localization of VTI11, its role in lytic vacuole trafficking and the recent observation that the *zig-1* phenotype is largely dependent on retromer-mediated resorting [23–26,31]. CLV1 has been shown to interact in the yeast two-hybrid system with a sorting nexin, a critical component of the retromer recycling complex [32–34]. In addition, it has been shown that blocking lysosomally targeted cargo in animal systems can also induce sorting into the recycling pathway [35]. It remains to be determined if CLV1 is an actual cargo for retromer or VTI11-dependent trafficking

We would expect that CLV1 undergoes endocytosis from the PM prior to trafficking to the vacuole. Despite several attempts we were unable to visualize any intermediate locations between the PM and vacuole accumulation. It is possible that any endosomes mediating this traffic are transient and smaller in diameter than Golgi vesicles. It should be noted that we were also unable to see any VHAa1-RFP signal, which labels the early endosome/TGN, in

the IM of Arabidopsis (data not shown) nor were we able to resolve Rab C1 YFP-labeled compartments beyond a background glow (wave 3, wave collection, [36]), despite robust imaging of these compartments in root tissues (data not shown).

It has been demonstrated that, while transient *CLV3* signaling downregulates *WUS*, sustained *CLV3* often results in reactivation of *WUS* [4]. In addition, *CLV3* levels can be manipulated over a wide range and still result in apparently wild type plants [4]. Thus the perception and response to CLV3 is buffered within the growing meristem. Cytokinin regulation of *WUS* or RLKs which counter act CLV1 may provide buffering activity [37,38]. Ligand-induced trafficking and degradation of CLV1 could also provide a mechanism for this buffering.

Experimental Procedures

Plant Material

clv1-11 [21], *clv2-1* [16], and *clv3-2* [22] were described previously and are all in the Landsberg-erecta genetic background. *clv1-101* is a fully recessive T-DNA insertion mutant in the Columbia background and was obtained from the from the ABRC (WiscDsLox489-492B1 [15]). The VAC-RFP lines corresponds to the spL-RFP lines described in [39]. See Supplemental Material and Methods for additional methods.

Construction of vectors

Details of vector construction are provided in Supplemental Experimental Proceedures.

Confocal microscopy

Microscopy was performed on freshly detached lateral inflorescences as previously described as in [40]. Young IMs were used in which developing flowers had not yet opened. Tissue from this remains viable for several hours [40] but were imaged immediately following detachment. The tissue was imaged using a 63X dipping lens. GFP and chlorophyll were stimulated using a 488 nm laser at 18.9% activation. A 505–550 bandpass filter for GFP and 585 longpass filter was used for chlorophyll detection. The 505–550 filter was used to maximize GFP signal collection. Additional details, including dye staining are provided in Supplemental Experimental Procedures.

Protein Extraction and Analysis

10 lateral inflorescence meristems were removed and unopened flowers were dissected off. Fresh tissue was ground in extraction buffer (10 mM Hepes pH 7.4, 0.2 mM EDTA, 2mM $MgCl_2$, 0.1 M NaCl, 10% Glycerol, 1% Triton X-100, 1 mM PMSF) containing PhosphoStop and Protease Complete tablets (Roche). Samples were incubated with gentle rotation at 4 °C overnight. Samples were spun 10 minutes, supernatant was quantified using BioRad protein quantification kit and the remaining sample was diluted into 6× Laemmli Buffer. Proteins were separated on a 8% SDS Page gel, blotted and probed with anti-GFP (Roche).

Supplementary Material

Refer to Web version on PubMed Central for supplementary material.

Acknowledgments

We thank Dr. Philippa Barrell for kindly providing the MOA binary series of vectors. We thank Dr. Natasha Raikhel for providing the *zig-1* seed. We thank Dr. Lorenzo Frigerio for providing the VAC-RFP seed line. We

thank the ABRC for providing seed stocks. We thank Arnavaz Garda for her excellent technical assistance. We also thank members of the Meyerowitz lab for help with imaging techniques and manuscript comments. This work was funded by NIH National Research Service Award F32 GM080843 to ZLN, NIH National Research Service Award F32 GM075460 to XQ, NIH National Research Service Award F32 GM090534 to PT, and NIH grant 1R01 GM086639 to EMM.

REFERENCES

1. Wang G, Fiers M. CLE peptide signaling during plant development. Protoplasma. 2009; 240:33–43. [PubMed: 20016993]
2. Brand U, Fletcher JC, Hobe M, Meyerowitz EM, Simon R. Dependence of stem cell fate in Arabidopsis on a feedback loop regulated by CLV3 activity. Science. 2000; 289:617–619. [PubMed: 10915624]
3. Clark SE, Running MP, Meyerowitz EM. CLAVATA3 is a specific regulator of shoot and floral meristem development affecting the same processes as CLAVATA1. Development. 1995; 121:2057–2067.
4. Muller R, Borghi L, Kwiatkowska D, Laufs P, Simon R. Dynamic and compensatory responses of Arabidopsis shoot and floral meristems to CLV3 signaling. Plant Cell. 2006; 18:1188–1198. [PubMed: 16603652]
5. Lenhard M, Laux T. Stem cell homeostasis in the Arabidopsis shoot meristem is regulated by intercellular movement of CLAVATA3 and its sequestration by CLAVATA1. Development. 2003; 130:3163–3173. [PubMed: 12783788]
6. Barton MK. Twenty years on: The inner workings of the shoot apical meristem, a developmental dynamo. Dev Biol. 2009
7. Rojo E, Sharma VK, Kovaleva V, Raikhel NV, Fletcher JC. CLV3 is localized to the extracellular space, where it activates the Arabidopsis CLAVATA stem cell signaling pathway. Plant Cell. 2002; 14:969–977. [PubMed: 12034890]
8. Ohyama K, Shinohara H, Ogawa-Ohnishi M, Matsubayashi Y. A glycopeptide regulating stem cell fate in Arabidopsis thaliana. Nat Chem Biol. 2009; 5:578–580. [PubMed: 19525968]
9. Kondo T, Sawa S, Kinoshita A, Mizuno S, Kakimoto T, Fukuda H, Sakagami Y. A plant peptide encoded by CLV3 identified by in situ MALDI-TOF MS analysis. Science. 2006; 313:845–848. [PubMed: 16902141]
10. Clark SE, Williams RW, Meyerowitz EM. The CLAVATA1 gene encodes a putative receptor kinase that controls shoot and floral meristem size in Arabidopsis. Cell. 1997; 89:575–585. [PubMed: 9160749]
11. Ogawa M, Shinohara H, Sakagami Y, Matsubayashi Y. Arabidopsis CLV3 peptide directly binds CLV1 ectodomain. Science. 2008; 319:294. [PubMed: 18202283]
12. Schoof H, Lenhard M, Haecker A, Mayer KF, Jurgens G, Laux T. The stem cell population of Arabidopsis shoot meristems in maintained by a regulatory loop between the CLAVATA and WUSCHEL genes. Cell. 2000; 100:635–644. [PubMed: 10761929]
13. Miwa H, Betsuyaku S, Iwamoto K, Kinoshita A, Fukuda H, Sawa S. The receptor-like kinase SOL2 mediates CLE signaling in Arabidopsis. Plant Cell Physiol. 2008; 49:1752–1757. [PubMed: 18854335]
14. Muller R, Bleckmann A, Simon R. The receptor kinase CORYNE of Arabidopsis transmits the stem cell-limiting signal CLAVATA3 independently of CLAVATA1. Plant Cell. 2008; 20:934–946. [PubMed: 18381924]
15. Kinoshita A, Betsuyaku S, Osakabe Y, Mizuno S, Nagawa S, Stahl Y, Simon R, Yamaguchi-Shinozaki K, Fukuda H, Sawa S. RPK2 is an essential receptor-like kinase that transmits the CLV3 signal in Arabidopsis. Development. 2010; 137:3911–3920. [PubMed: 20978082]
16. Jeong S, Trotochaud AE, Clark SE. The Arabidopsis CLAVATA2 gene encodes a receptor-like protein required for the stability of the CLAVATA1 receptor-like kinase. Plant Cell. 1999; 11:1925–1934. [PubMed: 10521522]
17. Kayes JM, Clark SE. CLAVATA2, a regulator of meristem and organ development in Arabidopsis. Development. 1998; 125:3843–3851. [PubMed: 9729492]

18. Geldner N, Hyman DL, Wang X, Schumacher K, Chory J. Endosomal signaling of plant steroid receptor kinase BRI1. Genes Dev. 2007; 21:1598–1602. [PubMed: 17578906]
19. Wiley HS, Burke PM. Regulation of receptor tyrosine kinase signaling by endocytic trafficking. Traffic. 2001; 2:12–18. [PubMed: 11208164]
20. Murphy JE, Padilla BE, Hasdemir B, Cottrell GS, Bunnett NW. Endosomes: a legitimate platform for the signaling train. Proc Natl Acad Sci U S A. 2009; 106:17615–17622. [PubMed: 19822761]
21. Dievart A, Dalal M, Tax FE, Lacey AD, Huttly A, Li J, Clark SE. CLAVATA1 dominant-negative alleles reveal functional overlap between multiple receptor kinases that regulate meristem and organ development. Plant Cell. 2003; 15:1198–1211. [PubMed: 12724544]
22. Fletcher JC, Brand U, Running MP, Simon R, Meyerowitz EM. Signaling of cell fate decisions by CLAVATA3 in Arabidopsis shoot meristems. Science. 1999; 283:1911–1914. [PubMed: 10082464]
23. Surpin M, Zheng H, Morita MT, Saito C, Avila E, Blakeslee JJ, Bandyopadhyay A, Kovaleva V, Carter D, Murphy A, et al. The VTI family of SNARE proteins is necessary for plant viability and mediates different protein transport pathways. Plant Cell. 2003; 15:2885–2899. [PubMed: 14615598]
24. Sanmartin M, Ordonez A, Sohn EJ, Robert S, Sanchez-Serrano JJ, Surpin MA, Raikhel NV, Rojo E. Divergent functions of VTI12 and VTI11 in trafficking to storage and lytic vacuoles in Arabidopsis. Proc Natl Acad Sci U S A. 2007; 104:3645–3650. [PubMed: 17360696]
25. Niihama M, Uemura T, Saito C, Nakano A, Sato MH, Tasaka M, Morita MT. Conversion of functional specificity in Qb-SNARE VTI1 homologues of Arabidopsis. Curr Biol. 2005; 15:555–560. [PubMed: 15797025]
26. Uemura T, Ueda T, Ohniwa RL, Nakano A, Takeyasu K, Sato MH. Systematic analysis of SNARE molecules in Arabidopsis: dissection of the post-Golgi network in plant cells. Cell Struct Funct. 2004; 29:49–65. [PubMed: 15342965]
27. Clark SE, Running MP, Meyerowitz EM. CLAVATA1, a regulator of meristem and flower development in Arabidopsis. Development. 1993; 119:397–418. [PubMed: 8287795]
28. Geier F, Lohmann JU, Gerstung M, Maier AT, Timmer J, Fleck C. A quantitative and dynamic model for plant stem cell regulation. PLoS One. 2008; 3:e3553. [PubMed: 18958283]
29. Ivanov R, Gaude T. Endocytosis and endosomal regulation of the S-receptor kinase during the self-incompatibility response in Brassica oleracea. Plant Cell. 2009; 21:2107–2117. [PubMed: 19622804]
30. Yadav RK, Fulton L, Batoux M, Schneitz K. The Arabidopsis receptor-like kinase STRUBBELIG mediates inter-cell-layer signaling during floral development. Dev Biol. 2008; 323:261–270. [PubMed: 18771664]
31. Hashiguchi Y, Niihama M, Takahashi T, Saito C, Nakano A, Tasaka M, Morita MT. Loss-of-Function Mutations of Retromer Large Subunit Genes Suppress the Phenotype of an Arabidopsis zig Mutant That Lacks Qb-SNARE VTI11. Plant Cell. 2010
32. Vanoosthuyse V, Tichtinsky G, Dumas C, Gaude T, Cock JM. Interaction of calmodulin, a sorting nexin and kinase-associated protein phosphatase with the Brassica oleracea S locus receptor kinase. Plant Physiol. 2003; 133:919–929. [PubMed: 14555783]
33. Jaillais Y, Fobis-Loisy I, Miege C, Rollin C, Gaude T. AtSNX1 defines an endosome for auxin-carrier trafficking in Arabidopsis. Nature. 2006; 443:106–109. [PubMed: 16936718]
34. Kleine-Vehn J, Leitner J, Zwiewka M, Sauer M, Abas L, Luschnig C, Friml J. Differential degradation of PIN2 auxin efflux carrier by retromer-dependent vacuolar targeting. Proc Natl Acad Sci U S A. 2008; 105:17812–17817. [PubMed: 19004783]
35. Raiborg C, Malerod L, Pedersen NM, Stenmark H. Differential functions of Hrs and ESCRT proteins in endocytic membrane trafficking. Exp Cell Res. 2008; 314:801–813. [PubMed: 18031739]
36. Geldner N, Denervaud-Tendon V, Hyman DL, Mayer U, Stierhof YD, Chory J. Rapid, combinatorial analysis of membrane compartments in intact plants with a multicolor marker set. Plant J. 2009; 59:169–178. [PubMed: 19309456]

37. DeYoung BJ, Bickle KL, Schrage KJ, Muskett P, Patel K, Clark SE. The CLAVATA1-related BAM1, BAM2 and BAM3 receptor kinase-like proteins are required for meristem function in Arabidopsis. Plant J. 2006; 45:1–16. [PubMed: 16367950]

38. Gordon SP, Chickarmane VS, Ohno C, Meyerowitz EM. Multiple feedback loops through cytokinin signaling control stem cell number within the Arabidopsis shoot meristem. Proc Natl Acad Sci U S A. 2009; 106:16529–16534. [PubMed: 19717465]

39. Hunter PR, Craddock CP, Di Benedetto S, Roberts LM, Frigerio L. Fluorescent reporter proteins for the tonoplast and the vacuolar lumen identify a single vacuolar compartment in Arabidopsis cells. Plant Physiol. 2007; 145:1371–1382. [PubMed: 17905861]

40. Reddy GV, Heisler MG, Ehrhardt DW, Meyerowitz EM. Real-time lineage analysis reveals oriented cell divisions associated with morphogenesis at the shoot apex of Arabidopsis thaliana. Development. 2004; 131:4225–4237. [PubMed: 15280208]

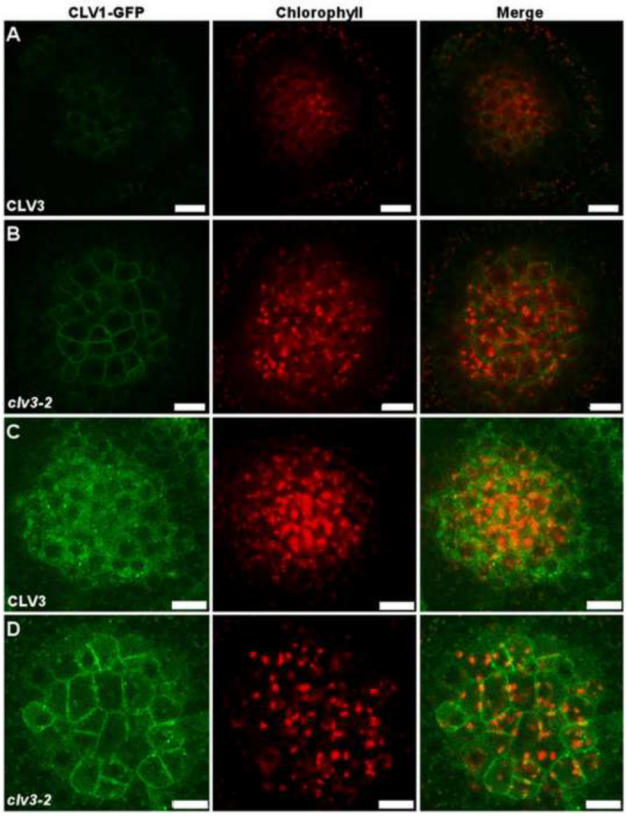

Figure 1. CLV1 accumulates at the plasma membrane in *clv3-2* plants

Images represent single *clv1-11 CLV1::CLV1-2xGFP* transgenic line introgressed into *clv1-11 clv3-2* plants. Images are of L3/L4 cell layer of young IMs (see text). A and B rows are an average of four scans. C and D rows are a sum of four scans to highlight GFP signal. See Supplemental figures for imaging controls. Scale bar, 10 μm.

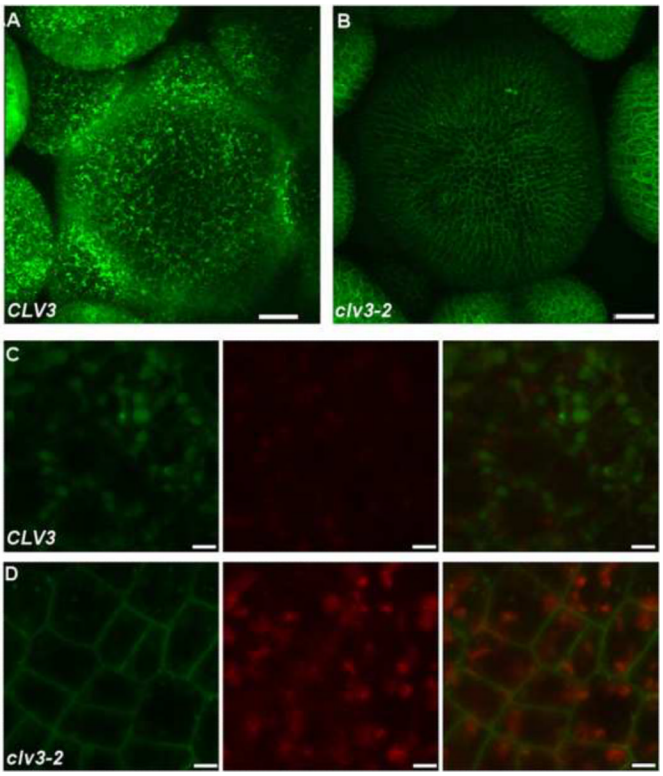

Figure 2. CLV1 traffics to the vacuole in a CLV3-dependent manner

Images from an introgression of a single *pUBQ::CLV1-2xGFP* transgenic line in the *clv1-101* background into *clv1-11 clv3-2* plants (see text). Images are of A) *CLV3 ER* and B) *clv3-2 ER* plants. Images represent reconstructed stack of young IMs. Scale bar, 20 μm. C and D, detail images from a separate introgression of a different *UBQ::CLV1-2xGFP* transgenic line in the *clv1-11 er* background into the genotype *clv1-11 clv3-2 er*. Images are of the L1 epidermal cell layer and represent and average of four scans. Scale bars, 2 μm.

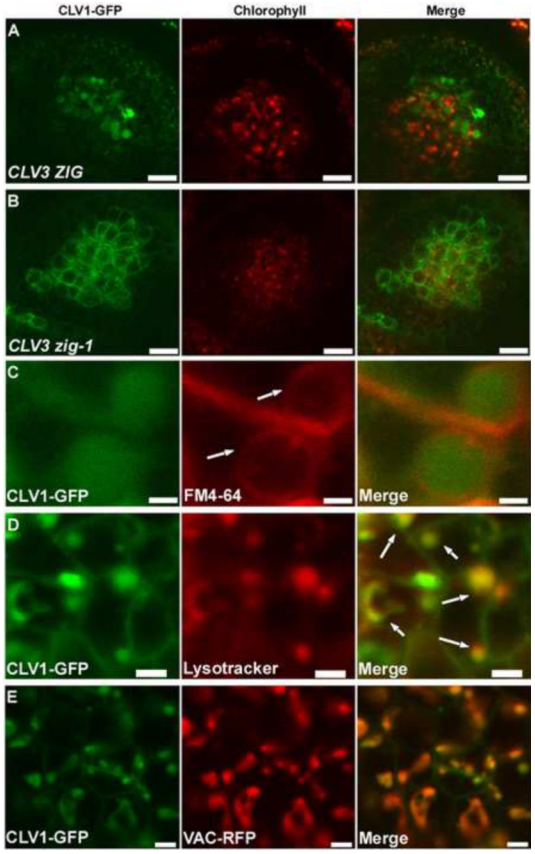

Figure 3. CLV1 traffics to the lytic vacuole in a VTI11 dependent manner

Images of L3 cells of young IMs from an introgression of *pCLV1::CLV1-2xGFP clv1-11* into the *clv1-11 clv3-2 zig-1* triple mutant background (see text). Row A: Scan of L3 cells from IM of *pCLV1::CLV1-2xGFP CLV3 ZIG*. Row B: Scan of L3 cells from *pCLV1::CLV1-2xGFP CLV3 zig-1*. Images are a sum of 4 scans. Scale bars, 10 μm. Row C: Confocal image of IM L1 cells from *pUBQ::CLV1-2xGFP CLV3* plant stained for 3 hrs with FM4-64. Arrows indicate FM4-64 localization to the tonoplast surrounding the CLV1-2xGFP signal. Images are an average of 4 scans. Scale Bars, 1 mm. Row D: Confocal image of IM L1 cells from *pUBQ::CLV1-2xGFP CLV3* plant stained for 5 minutes with LysoTracker Red. Arrows indicate areas of colocalization between CLV1-2xGFP and LysoTracker Red in vacuoles. Images are an average of 4 scans. Scale Bars, 2 2 μm. Row E: Confocal image of IM L1 cells from *pUBQ::CLV1-2xGFP VAC-RFP CLV3* plants. Scale Bars, 2 2 μm. Images are an average of 2 scans.

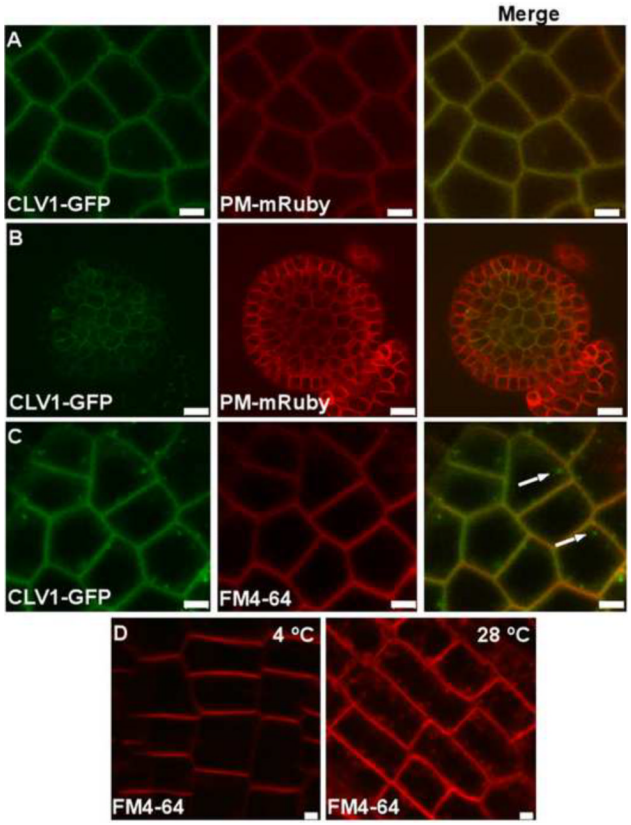

Figure 4. CLV1 localizes to the plasma membrane in *clv3* plants

Row A: CLV1-2xGFP colocalizes with PM-mRUBY in *clv3-2* plants. Confocal image of IM L1 cells from *pUBQ::CLV1-2xGFP* pUBQ:PM-2xmRUBY *clv3-2*. Images are an average of 4 scans. Scale bars, 10 μm. Row B: CLV1-2xGFP expressed from the *pCLV1::CLV1-2xGFP* transgene in a *pUBQ:PM-2xmRUBY clv3-2* FM colocalizes with PM-2xmRUBY. Images are an average of 4 scans. Scale bars, 10 μm.. Row C: CLV1 colocalizes with FM4-64 at the PM in cold treated IMs. Arrows indicate CLV1-GFP vesicles lacking FM4-64 signal. Row D: Cold treatment abolishes FM4-64 endocytosis in root cells. Seedling roots were incubated for 1 hr with FM4-64 at 4°C or 20 minutes at 28°C. Note the lack of FM4-64 positive vesicles at 4°C.

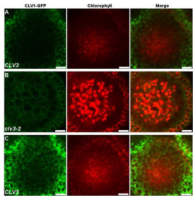

Figure 5. High levels of CLV1 in L1 and L2 fail to prevent CLV3-dependent trafficking of CLV1 in L3 cells

A and B, images taken from L3 cells of young IMs from the *clv1-11 UBQ::CLV1-2xGFP* introgression into the *clv3-2 clv1-11* background. A and B represent an average of four scans. C, a sum of four scans from *CLV3* progeny to highlight weak signals in the L3 cells.

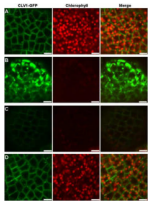

Figure 6. CLV3 is sufficient to drive CLV1 downregulation at the plasma membrane and trafficking to the lytic vacuole

Inducible expression of *CLV3* restores vacuolar trafficking of CLV1-2xGFP. Images are derived from F1 progeny of a cross between *clv3-2 DEX::CLV3* and *clv3-2 UBQ::CLV1-2xGFP* plants. A, Image taken from young IMs from an F1 plant before application of dexamethasone (DEX). Note the robust accumulation of CLV1-2xGFP on the PM. B, different IM from the same F1 plant following 3 days of spraying with 20 μm DEX. Note the strong vacuolar accumulation of GFP signal. C, a different IM from the same DEX treated plant displaying greatly reduced levels of CLV1-2xGFP at the PM. D, an IM taken from a control treated F1 plant at the same time as B and C. Images represent a sum of 4 scans. Scale bars, 5 μm.

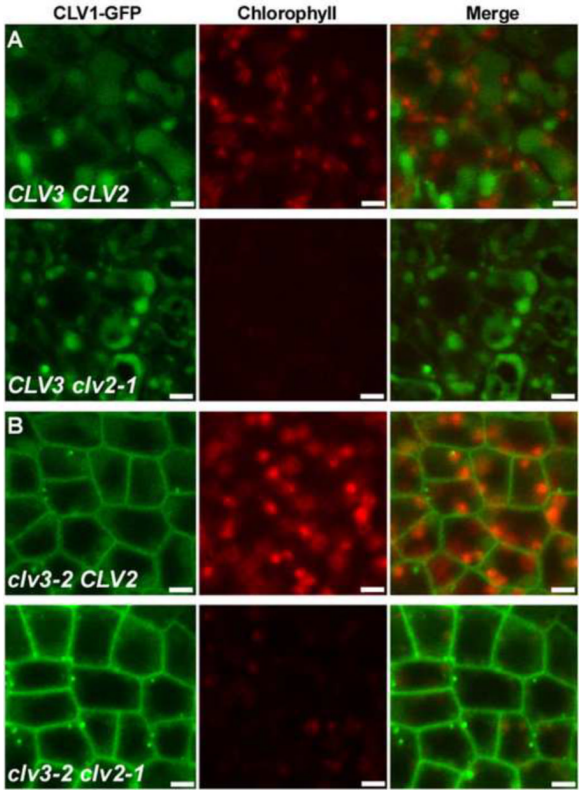

Figure 7. *CLV2* is not required for CLV1 trafficking or stability

CLV1-2xGFP traffics to the lytic vacuole independent of *CLV2*. Image of L1 tissue from *pUBQ::CLV1-2xGFP* plants introgressed into the *CLV2* (upper) or *clv2-1* (lower) background. Image represents average of four scans. Scale bars, 2 μm. B). CLV1-2xGFP stability in *clv3-2* plants is not compromised in *clv2-1* plants. Image of L1 cells in young IMs from an introgression of *pUBQ::CLV1-2xGFP* into the *clv3-2 CLV2* (upper) or *clv3-2 clv2-1* (lower) backgrounds. Image represents average of four scans. Scale bars, 2 μm.